Post-print of: Artichowicz W., Gąsiorowski D. (2018) Numerical Analysis of Steady Gradually Varied Flow in Open Channel Networks with Hydraulic Structures. In: Kalinowska M., Mrokowska M., Rowiński P. (eds) Free Surface Flows and Transport Processes. GeoPlanet: Earth and Planetary Sciences. Springer, Cham. https://doi.org/10.1007/978-3-319-70914-7_6

Numerical analysis of steady gradually varied flow in open channel networks with hydraulic structures

Wojciech Artichowicz[1] and Dariusz Gąsiorowski[1]

Abstract In this paper, a method for numerical analysis of steady gradually varied flow in channel networks with hydraulic structures is considered. For this purpose, a boundary problem for the system of ordinary differential equations consisting of energy equation and mass conservation equations is formulated. The boundary problem is solved using finite difference technique which leads to the system of non-linear algebraic equations. The arising system is solved with modified Picard method. The presented methodology is applicable to any channel network type and any type of hydraulic structure.

1 Introduction

One-dimensional steady gradually varied flow (SGVF) in open channels is one of the most frequently considered flow types in hydraulic engineering. As it is one of the basic problems, it seems to be well recognized (Chow, 1959; Cunge et. al., 1978; French, 1978; Chanson, 2004; Szymkiewicz, 2010). However, practical modeling of this kind of flow in channel networks still remains an issue. In the literature, two approaches to this problem can be found. From formal viewpoint, both of them require formulation of the boundary problem for the governing equations describing SGVF. Both approaches have their advantages and drawbacks. One of the approaches is based on the shooting method. Such approach is, for example, implemented in HEC-RAS software (US Army Corps of Engineers, 2010).

---

[1] Wojciech Artichowicz (corresponding author), Dariusz Gąsiorowski

Gdansk University of Technology, Faculty of Civil and Environmental Engineering,

ul. G. Narutowicza 11/12, 80-233 Gdańsk, Poland

e-mail: wojartic@pg.gda.pl

However, this method has it difficult to converge in cases where looped channel networks are considered, which makes it useless for example for flow modelling in irrigation canals. Some improvements were introduced to this approach by Misra (1995, 1996, 1998) which allowed to work around the convergence problem. The second approach is based on the finite difference method (Schulte and Chaudhry, 1987; Szymkiewicz and Szymkiewicz, 2004). This approach offers an elegant mathematical formulation of the problem as well as unified description of the issue. In this approach, a global system of equations for the entire channel network is formulated. This method allows to perform computations for looped and dendric channel networks without distinction. However, it does not allow to perform simulations of the mixed flow regime, which is possible in the first case.

In this paper, the second approach is evaluated. The method introduced by Szymkiewicz and Szymkiewicz (2004) for SGVF modelling is adjusted for SGVF modelling in channel networks of any type, including hydraulic structures. This work is the expansion of the considerations presented in Szymkiewicz and Artichowicz (2016).

2 Governing equations

The modelling of the one-dimensional SGVF in open channels is based on the system of two ordinary differential equations derived from the system of the Saint-Venant equations (Artichowicz, 2015; Szymkiewicz, 2010):

$$\frac{dQ}{dx} = 0, \tag{1}$$

$$\frac{dE}{dx} = -S \tag{2}$$

where Q denotes the flow discharge, x is the spatial coordinate, E is the mechanical energy of the flow, and S is the energy slope. The first equation represents the mass conservation principle, whereas the second one represents the energy conservation principle. In the presented form the mass conservation equation states that no lateral flow is taken into consideration. However, including lateral inflow or outflow does not influence the presented solution methodology. The flow energy in Eq. (2) is expressed as follows

$$E = h + \frac{\alpha Q^2}{2gA^2}, \tag{3}$$

where h is the water stage level, α is the energy correctional coefficient, A is the active flow area and g is the gravitational acceleration. The energy slope can be estimated using Manning's formula:

$$S = \frac{n^2 Q^2}{A^2 R^{4/3}}, \tag{4}$$

in which n denotes the roughness coefficient and R is the hydraulic radius.

3 Boundary value problem for energy equation and its numerical solution with finite difference method

If flow discharge in a channel is known, then to obtain the flow profile it is necessary to formulate and solve the initial value problem for the energy equation. Such problem is a typical one and has been widely described in the literature (Cunge et. al., 1978; French, 1978; Szymkiewicz, 2010). However, if the flow discharge in a channel is unknown then, to find the water profile, a boundary problem for the system of ordinary differential Eqs. (1) and (2) has to be stated. Its solution provides the flow discharge value and flow profile in the considered channel (Fig. 1). To formulate the boundary problem for Eqs. (1) and (2) it is necessary to impose the boundary conditions at both ends of the considered channel reach. It means that water stage levels in the first (h_0) and the last (h_L) cross-section of the channel reach have to be imposed (Fig. 1).

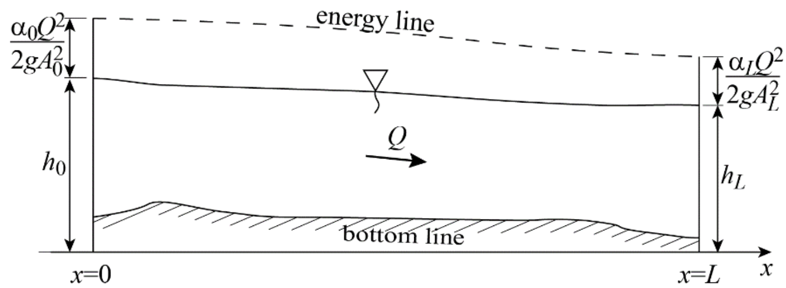

Fig. 1 Boundary problem for Eqs (1) and (2) in a channel reach.

The energy equation has to be approximated with numerical scheme. At least formally, the numerical solution of the boundary problem can be obtained by any numerical approach like collocation method, shooting method, finite difference method etc. In this work, the finite difference method (FDM) will be used. Application of the FDM to Eq. (2) yields:

$$\frac{E_{i+1} - E_i}{\Delta x_i} + \frac{1}{2}\left(S_i + S_{i+1}\right) = 0 \,. \tag{5}$$

In fact the FDM approximation is identical to implicit trapezoidal rule (Artichowicz and Prybytak, 2016; Ascher and Petzold, 1998). Substitution of Eqs. (3) and (4) into Eq. (5) yields:

$$-\left(h_i + \frac{\alpha_i Q^2}{2g A_i^2}\right) + \left(h_{i+1} + \frac{\alpha_{i+1} Q^2}{2g A_{i+1}^2}\right) + \frac{\Delta x_i}{2}\left(\frac{Q^2 n_i^2}{A_i^2 R_i^{4/3}} + \frac{Q^2 n_{i+1}^2}{A_{i+1}^2 R_{i+1}^{4/3}}\right) = 0 \,. \tag{6}$$

This form of the equation allows to consider the flow in one direction only. However, when channel networks are considered it is sometimes impossible to assume the proper flow directions in all of the network branches. To work around this problem, Eq. (6) can be rewritten in another form:

$$-\left(h_i + \frac{\alpha_i Q^2}{2g A_i^2}\right) + \left(h_{i+1} + \frac{\alpha_{i+1} Q^2}{2g A_{i+1}^2}\right) + \frac{Q\,|\,Q\,|\,\Delta x_i}{2}\left(\frac{n_i^2}{A_i^2 R_i^{4/3}} + \frac{n_{i+1}^2}{A_{i+1}^2 R_{i+1}^{4/3}}\right) = 0 \,. \tag{7}$$

Substituting the square of the flow discharge in the energy slope term with the product of the discharge and its absolute value allows to include the direction of the flow with sign of the discharge value. If the value is positive, it means that the flow occurs in the assumed direction; if the sign is negative, the flow occurs in the direction opposite to the assumed one. The assumed flow direction is from the cross-section 1 (x=0) to M (x=L).

The idea of the FDM is to divide the channel into M computational sections (Fig. 2) and to write Eq. (7) for each of them.

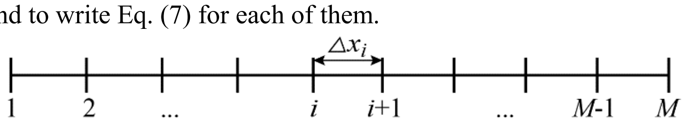

Fig. 2 A computational schematic of the channel.

The resulting system of equations will have M-1 equations and M+1 unknowns. Necessary additional equations arise from the imposed boundary values in the first and last cross-sections:

$$h_1 = h_0 \text{ and } h_M = h_L \,. \tag{8a,b}$$

The resulting system of non-linear algebraic equations can be written in the short form as

$$\mathbf{Ax} = \mathbf{b} \,. \tag{9}$$

The structure of the system (9) is presented in Eq. (10).

$$\begin{bmatrix} a_{1,1} & & & & & & & \\ a_{2,1} & a_{2,2} & & & & & & a_{2,M+1} \\ & \ddots & \ddots & & & & & \vdots \\ & & a_{i,i-1} & a_{i,i} & & & & a_{i,M+1} \\ & & & \ddots & \ddots & & & \vdots \\ & & & & & a_{M-1,M} & a_{M,M} & a_{M,M+1} \\ & & & & & & a_{M+1,M} & \end{bmatrix} \begin{Bmatrix} h_1 \\ \vdots \\ h_i \\ h_{i+1} \\ \vdots \\ h_M \\ Q \end{Bmatrix} = \begin{Bmatrix} h_0 \\ 0 \\ \vdots \\ 0 \\ \vdots \\ 0 \\ h_L \end{Bmatrix}. \tag{10}$$

The elements of this system are as presented below. The first and last rows correspond to the imposed boundary conditions, so the elements values will be

$$a_{1,1} = 1 \text{ and } a_{M+1,M} = 1, \tag{11a,b}$$

whereas other elements are resulting from Eq. (7):

$$a_{i,i-1} = -1,\ a_{i,i} = 1,$$
$$a_{i,M+1} = \frac{Q}{2g}\left(-\frac{\alpha_i}{A_i^2} + \frac{\alpha_{i+1}}{A_{i+1}^2}\right) + \frac{|Q|\,\Delta x_i}{2}\left(\frac{n_i^2}{A_i^2 R_i^{4/3}} + \frac{n_{i+1}^2}{A_{i+1}^2 R_{i+1}^{4/3}}\right). \tag{12a,b,c}$$

The elements of the unknown vector are

$$x_i = h_i, \text{ and } x_{M+1} = Q, \tag{13a,b}$$

for i=1, ..., M. The elements of the right-hand side vector are equal to

$$b_1 = h_0,\ b_i = 0, \text{ and } b_{M+1} = h_L, \tag{14a,b,c}$$

The obtained system of equations (10) is an algebraic non-linear one. It can be successively solved using modified Picard method (Szymkiewicz and Szymkiewicz, 2004). Let us rewrite Eq. (9) in a form introducing iteration index k:

$$\mathbf{A}^*\mathbf{x}^{(k+1)} = \mathbf{b}, \tag{15}$$

where the modified system matrix $\mathbf{A}^*$ is computed based on the mean values of two previous iterations of the solution vector:

$$\mathbf{A}^* = \mathbf{A}\left(\frac{\mathbf{x}^{(k-1)} + \mathbf{x}^{(k)}}{2}\right). \tag{16}$$

In the first iteration (for k=0), the matrix is computed based on the starting point only $\mathbf{x}^{(0)}$:

$$\mathbf{A}^* = \mathbf{A}\left(\mathbf{x}^{(k)}\right). \tag{17}$$

The iterative process is considered as finished when the following criteria are fulfilled:

$$|\, h_i^{(k+1)} - h_i^{(k)} \,| < \varepsilon_h, \ \text{and} \ |\, Q^{(k+1)} - Q^{(k)} \,| < \varepsilon_Q, \tag{18a,b}$$

for i=1, 2, ..., M, where ε_h and ε_Q are the required solution accuracies of water stage levels and flow discharge, respectively.

5 Including the hydraulic structures

The method presented in the previous section can be applied to a channel with one or multiple hydraulic structures as well. An example of such a channel is presented in Fig. 3.

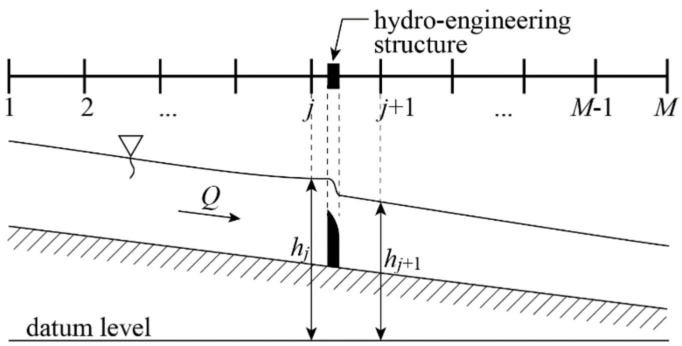

Fig. 3 The top view and longitudinal cross-sectional view to the schematic of the channel with hydraulic structure.

In such a situation, the elements of the system (10) corresponding to channel section with the hydraulic structure will be replaced. Instead of elements resulting from Eq. (7), the ones resulting from the formulas describing the hydraulic structure will be used. In general, such a formula can be written as

$$Q = Q(h_j, h_{j+1}), \tag{19}$$

meaning that water stage levels around the structure and the flow discharge are involved.

To include Eq. (19) into system (9) it has to be rearranged to a form allowing the extraction of the unknown water stage levels and flow discharge into the vector of unknowns **x**. The rearrangement will be presented on the examples of two most common hydraulic structures: weir and orfice.

4.1 Weir

The hydraulic scheme for submerged weir is presented in Fig. 4.

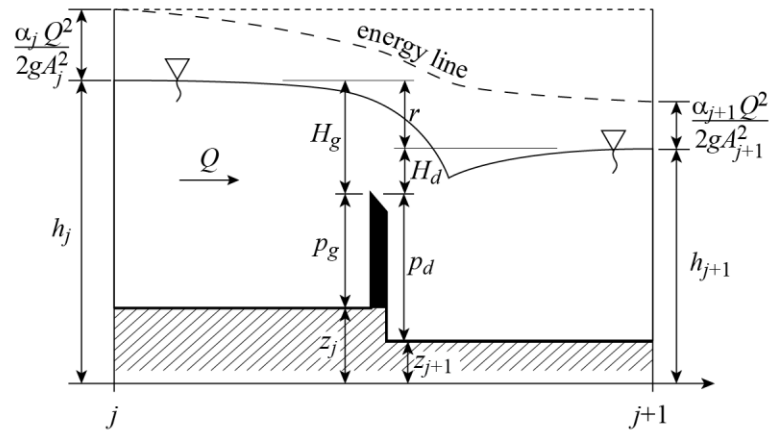

Fig. 4 The computational scheme for weir discharge computations.

In literature there are many formulas for estimating flow discharge of such structures as weirs. For simplicity let us consider rectangular sharp-crested weir. Expression for the discharge of such weir is

$$Q = \frac{2}{3}\mu B\sqrt{2g}\left[\left(H_g + \frac{\alpha_j Q^2}{2gA_j^2}\right)^{3/2} - \left(\frac{\alpha_j Q^2}{2gA_j^2}\right)^{3/2}\right]\cdot\sigma, \tag{20}$$

where μ is the weir discharge coefficient, H_g the water level above the crest before the weir, p_g the crest level over the bottom before the weir, B the weir width, and σ is the submersion coefficient, which can be expressed as (Kubrak and Kubrak, 2010)

$$\sigma = 1.05\left(1+0.02\frac{H_d}{p_d}\right)\sqrt[3]{\frac{H_g - H_d}{H_g}}\ , \tag{21}$$

in which H_d is the water level above the crest behind the weir, and p_d is the crest level over the bottom behind the weir.
Formula (20) is valid if $0.25<(H_g\text{-}H_d/p_d)<0.75$. If the weir is not submerged, then the value of the coefficient is taken as σ=1.

To include Eq. (20) into system of Eqs. (9) it has to be rearranged in such way that it will be possible to extract from it h_j, h_{j+1} and Q into the vector of unknowns. If the weir is not submerged, the rearranged Eq. (20) will take the form:

$$-Uh_j + Q = U\left(\frac{\alpha_j Q^2}{2gA_j^2} - z_j - p_g\right) - W\ , \tag{22}$$

where

$$U = \frac{2}{3}\mu B\sqrt{2g\left(H_g + \frac{\alpha_j Q^2}{2gA_j^2}\right)}\ ,$$

$$W = \frac{2}{3}\mu B\sqrt{2g}\left(\frac{\alpha_j Q^2}{2gA_j^2}\right)^{3/2}\ .$$

In such case, the resulting matrix and right-hand side vector will be expressed with the following formulas:

$$a_{j,j} = -U\ ,\ a_{j,j+1} = 0\ ,\ a_{j,M+1} = 1, \tag{23a,b,c}$$

$$b_j = U\left(\frac{\alpha_j Q^2}{2gA_j^2} - z_j - p_g\right) - W\ , \tag{24}$$

If the weir is submerged, Eq. (20) will be written as follows:

$$-\sigma U h_j - \left(T\frac{0.021}{p_d}\sqrt[3]{\frac{r}{H_g}}\right)h_{j+1} + Q = T\left(1.0291 - 0.021\frac{z_{j+1}}{p_d}\right)\sqrt[3]{\frac{r}{H_g}}\ , \tag{25}$$

with

$$T = U\left(\frac{\alpha_j Q^2}{2gA_j^2} - z_j - p_g\right) - W \cdot$$

In such a situation, the resulting matrix and right-hand side vector will be expressed with the following formulas:

$$a_{j,j} = -\sigma U\ , \ a_{j,j+1} = -T\,\frac{0.021}{p_d}\sqrt[3]{\frac{r}{H_g}}\ , \quad a_{j,M+1} = 1, \tag{26a,b,c}$$

$$b_j = T\left(1.0291 - 0.021\frac{z_{j+1}}{p_d}\right)\sqrt[3]{\frac{r}{H_g}}\ . \tag{27}$$

If necessary, it is possible to include the variability of the weir coefficient μ.

4.2 Unsubmerged orfice

Similarly as the weir, an orfice can be considered. The formula for the discharge of the small unsubmerged orfice is (Fig. 5):

$$Q = \mu A_o \sqrt{2gH_o}\ . \tag{28}$$

where μ is the orfice discharge coefficient, A_o the area of the orfice, H_o the water level above the centre of the orfice area, and p is the distance between the bottom and the bottom edge of the orfice.

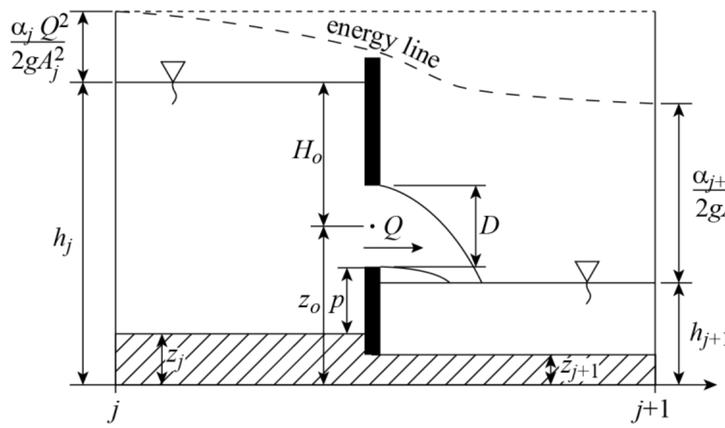

Fig. 5 The computational scheme for unsubmerged orfice discharge computations.

As previously, to include Eq. (28) in the system of Eqs. (9) it has to be rearranged. To this order, let us notice that in case of the circular or rectangular orfice it can be written that

$$z_o = z_j + p + \frac{D}{2}, \tag{29}$$

and

$$H_o = h_j - z_o. \tag{30}$$

To rearrange Eq. (28) for suitable form to be included in the system (9) it is convenient to raise its both sides to the power of two. Eq. (28), after rearrangement, will take the form:

$$Q^2 - 2g(\mu A_D)^2 h_j = -2g(\mu A_D)^2 z_o, \tag{31}$$

which leads to resulting matrix and right-hand side vector elements:

$$a_{j,j} = -2g(\mu A_D)^2,\ a_{j,j+1} = 0,\quad a_{j,M+1} = Q, \tag{32a,b,c}$$

$$b_j = -2g(\mu A_D)^2 z_o. \tag{33}$$

4.3 Submerged orfice

If the orfice is submerged, then the formula describing its discharge is (Fig. 6)

$$Q = \mu A_o \sqrt{2g\Delta H}\,, \tag{34}$$

where $\Delta H = h_j - h_{j+1}$ is the difference between the water level before and behind the orfice.

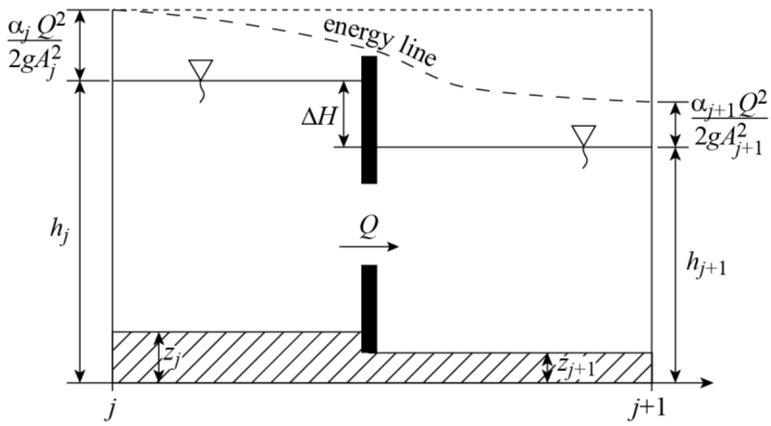

Fig. 6 The computational scheme for submerged orfice discharge computations.

As previously, it is convenient to raise both sides of formula (34) to the power of two:

$$Q^2 - 2g(\mu A_D)^2 h_j + 2g(\mu A_D)^2 h_{j+1} = 0\,. \tag{35}$$

The elements of the matrix and the right-hand side vector are

$$a_{j,j} = -2g(\mu A_D)^2,\; a_{j,j+1} = 2g(\mu A_D)^2,\quad a_{j,M+1} = Q\,, \tag{42a,b,c}$$

$$b_j = 0\,. \tag{36}$$

4.4 Example

To illustrate the FDM method and its accuracy let us consider a laboratory flume with adjustable bottom slope. The flume has the following parameters: length L=10 m, width B=0.38 m, bed slope s=0.001745. The Manning's roughness coefficient of the channel is constant and equal to n=0.0185 s m$^{-1/3}$. At the distance of x_{ovf}= 2.0 m, the sharp crested weir of height p_g=p_d =0.24 m is situated. The sketch of the laboratory station is presented in Fig. 10.

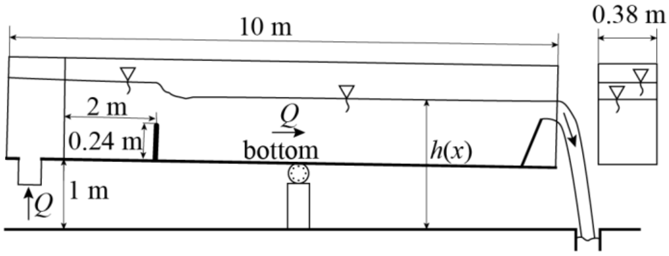

Fig. 7 The sketch of the laboratory flume.

The flow discharge was set to Q=0.0133 m^3 s^{-1}. The corresponding measured water stage levels at the first (x=0 m) and last (x=9 m) cross-sections were h_0=1.31 m, h_L=1.26 m, respectively. The above-mentioned FDM method was applied to simulate the flow in the flume. The initial discharge value was taken as Q_0= 0.01 m^3 s^{-1}. The initial water stage was taken as the stage corresponding to mean value of the depths resulting from the imposed boundary conditions. The weir discharge coefficient was computed using the following formula

$$\mu = 0.615\left(1 + \frac{1}{1000H_g + 1.6}\right)\left[1 + 0.5\left(\frac{H_g}{H_g + p_g}\right)^2\right]. \tag{37}$$

The computations required 6 iterations to finish with demanded accuracy ε_h = 0.0001 m and ε_Q=0.0001 m^3 s^{-1}. The obtained flow discharge value is Q_c=0.0142 m^3 s^{-1}, which means the relative error ε=$|Q$-$Q_c|/Q\cdot$100%=6.76%. The outcome of the measurements and computations was presented in Fig. 8. The computed water stage levels are very similar to the measured values, which confirms the efficacy of the presented methodology.

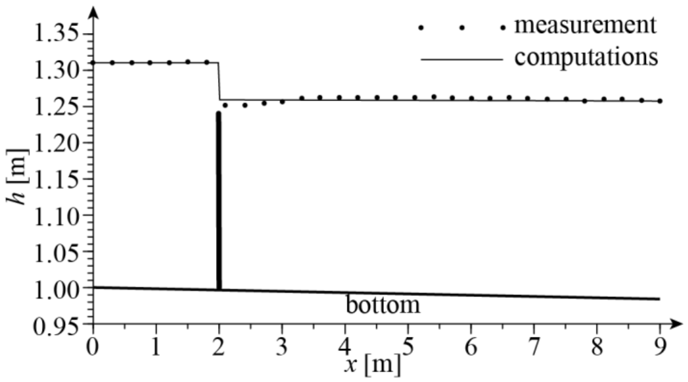

Fig. 8 The comparison of the measurements and computations outcome.

5 Channel networks

The presented methodology can be applied seamlessly to channel networks of any type. To perform the computations in such a case, each channel has to be divided into computational cross-sections in the same manner as presented in the case of the single channel. However, to close the arising system of equations, additional equations are required. Those equations are representations of the mass conservation principle and the energy stage equality applied to junctions.

The scheme of the typical channel junction and its computational representation is displayed in Fig. 9.

Fig. 9 (a) The sketch of the channel junction and (b) its typical computational representation.

It is possible to include any number of channels in a junction representation, however, in practice, junctions with more than three channels are very rare. The equation representing the mass conservation principle is

$$\sum_{P} Q_P = 0 . \tag{38}$$

with P becoming the index of each channel included in the junction. For the situation presented in Fig. 9 it would mean that P=I, J, K. Equation (38) means that the volume of the water flowing into the junction and flowing out of the junction is identical. To include Eq. (38) in the arising global system of equations it is necessary to assume the flow directions in each channel of the considered network. The flow direction is then represented with the sign of the discharge value as previously mentioned. The equations representing the equality of the energy in the junction can be written as

$$h_i + \frac{\alpha_i Q_I^2}{2g A_i^2} = h_j + \frac{\alpha_j Q_J^2}{2g A_j^2} = h_k + \frac{\alpha_k Q_K^2}{2g A_k^2}, \tag{39}$$

which means that the flow energy in each of the cross sections included in junction is the same. Eq. (39) in fact represents two equations resulting from the situation presented in Fig. 9. In a general case in which P channels are included in the junction to express the equality of the energy in the junction P-1 equations will arise, where P means the number of channels included in the joint.

The resulting global system of equations will include subsystems written for each channel expressed by system (10) and from Eqs. (38) and (39) representing the junctions. If there are hydraulic structures in the channels included in the network they can be included in the model with the methodology described in section 4 without any changes. In each step of the computational process, the flow direction in the channels can change, which has to be taken into consideration when writing the equations describing the hydraulic structures. The resulting system of non-linear algebraic equations, as previously, can be solved using the modified Picard method.

5.1 Example

Let us consider an imaginary channel network consisting of eleven channels (Fig. 10). All channels in the network are rectangular and have width equal to B=5 m. Also roughness coefficient is identical in all channels and is equal to n=0.03 s m$^{-1/3}$. The bed slopes s and lengths L of the channels are given in Table 1. The channel network contains four identical rectangular weirs (denoted in Fig. 10 as *wr* 1-4 situated in channels 2, 3, 5 and 7). The parameters of the weirs have the following values: the width B_{wr}=5 m, the crest levels over the bottom p_g=p_d=1 m. The discharge μ_{wr} coefficient is computed using Eq. (37). The orfice parameters are: width B_{orf}=2.5 m, height D=0.3 m, discharge coefficient μ_{orf}=0.67, the bottom edge of the orfice is at the level of the channel bed thus p=0 m. The orfice is situated in channel 4. All hydraulic structures are positioned in the half of the channel lengths.

The network contains pairs of identical channels placed symmetrically: 2 and 3, 5 and 7, 9 and 10. The channel network is thus symmetrical with regard to the channels 1, 4 and 11.

The imposed boundary conditions are water stage levels corresponding to the given water depths H_{B1}= 2 m, H_{B2}= 1.2 m, H_{B3} =H_{B4}= 1.3 m. The imposed starting values for iterative process were the same for all the channels and were equal to $H^{(0)}$= 5 m and $Q^{(0)}$=0.1 m^3 s^{-1}. It took 16 iterations to obtain the demanded accuracy ε_h = 0.001 m and ε_Q=0.001 m^3 s^{-1}. The computed flow discharges are presented in Table 1.

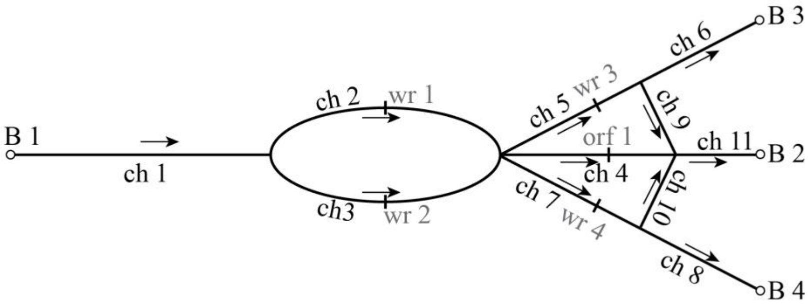

Fig. 10 The schematic of the considered channel network.

Table 1 The parameters of the channel network and the computed discharges.

No.	s [-]	L [m]	Q [m^3 s^{-1}]
1	0.0001	2000	5.502
2	0.0001	1000	2.751
3	0.0001	1000	2.751
4	0.0001	1500	1.087
5	0.0001333	1500	2.207
6	0.0001	1500	1.477
7	0.0001333	1500	2.207
8	0.0001	1500	1.477
9	- 0.00005	1000	0.730
10	- 0.00005	1000	0.730
11	0.0002	1000	2.547

The water profiles in paths consisting of channels 1-2-5-6, 4-11 and channel 9 are presented in Figs. 11, 12 and 13, respectively. As the network is symmetrical, the flow profiles in the remaining channels are identical as in the presented paths (Fig. 10).

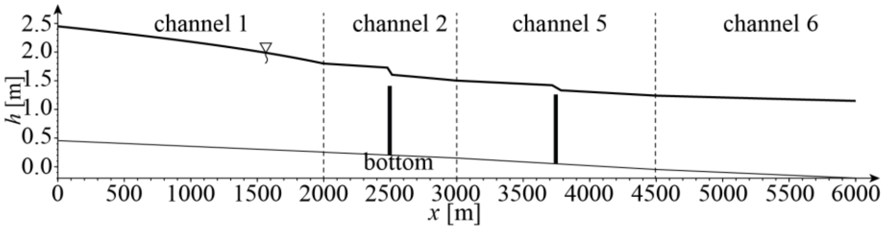

Fig. 11 The flow profile in the path connecting channels 1-2-5-6.

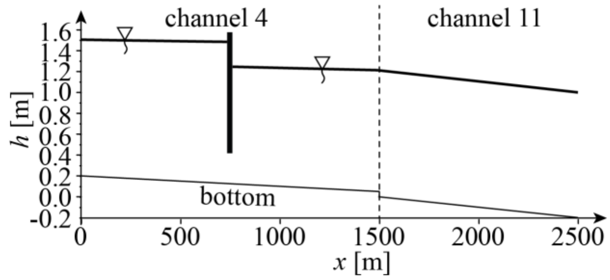

Fig. 12 The flow profile in the path connecting channels 4-11.

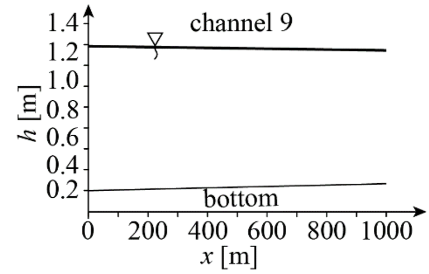

Fig. 13 The flow profile in channel 9.

7 Conclusions

In this paper, the methodology for SGVF modeling in channel networks with hydraulic structures of any type was presented. The core of the presented methodology is the system of ordinary differential equations consisting of the continuity and energy equations representing the one-dimensional SGVF in open channels. This system was approximated with finite difference method, which led to non-linear system of algebraic equations. If the network branches include hydraulic structures, the rows of this system corresponding to the cross-sections embracing the structures have to be modified. For such cross-sections the algebraic formulas involving discharge and water stage values before and behind the structure are used instead of the equations resulting from the approximation of the energy equation. The resulting system is closed by adding the equations representing the boundary conditions written for the pending cross-sections, and equations representing the energy line equality and mass conservation principle in the network junctions. The resulting system can be successively solved with modified Picard method.

The efficacy of this methodology was tested with imaginary examples as well as against experimental outcome.

References

Ascher U. M., Petzold L. R. (1998) Computer methods for Ordinary Differential Equations and Difference-Algebraic Equations, SIAM, Philadelphia.

Artichowicz W., Prybytak D. (2015) Impact of Energy Slope Averaging Methods on NumericalSolution of 1D Steady Gradually Varied Flow, Archives of Hydro-Engineering and Environmental Mechanics, Vol. 62 (2015), No. 3–4, pp. 101–119, Gdańsk 2015,DOI: 10.1515/heem-2015-0022

Chow V. T. Open-channel hydraulics, McGraw-Hill / Kogakusha Company LTD, Tokyo, 1959.

Cunge J. A., Holly F. M., Verwey A.: Practical aspects of computational river hydraulics, Pitman advanced publishing program, Boston, London, Melbourne 1979.

Dubin, J. R.: On gradually varied flow profiles in rectangular open channels, Journal of Hydraulic Research, 37: 1, 99 — 106, 1999 DOI: 10.1080/00221689909498534.

Jan, C.-D., Chen, C.-L., (2012) Use of the Gaussian hypergeometric function to solve the equation of gradually varied flow. Journal of Hydrology, 456–457, 139–145.

Kubrak E., Kubrak J. (2010) Podstawy obliczeń z mechaniki płynów w inżynierii i ochronie środowiska. SGGW, Warszawa.

Misra R., (1995) Steady flow simulation in irrigation canals. SADHANA Academy proceedings in engineering sciences. vol. 20, Part 6, pp. 955-969.

Misra R., (1996) Spatially varied steady flow in irrigation canals, Agricultural Water Management, Vol. 30, p.217-235.

Misra R., (1998) Recursive algorithm for steady flow in a canal network. Advances in Engineering Software, Vol. 29. No. 1, pp. 77-86, 1998.

Schulte A. M., Chaudhry M. H., (1987) Gradually-varied flows in open channel networks, Journal of Hydraulic Research, Vol. 25, No 3;

Szymkiewicz R., (2010) Numerical modeling in open channel hydraulics. Springer.

Szymkiewicz A, Szymkiewicz R, (2004): Method to solve the non-linear systems of equations for steady gradually varied flow in open channel network, Communications in numerical methods in engineering, Vol. 20, No 4.

Szymkiewicz R., Artichowicz W. (2016) Modelowanie przepływu ustalonego niejednostajnego w sieciach kanałów otwartych z uwzględnieniem obiektów hydrotechnicznych. A chapter in monography: Modelowanie przepływów w ośrodkach porowatych oraz w sieciach rzecznych, Ed: Sroka Z, Tschuschke W., Bogucki Wydawnictwo Naukowe, Poznań.

Todisco M.T., (2009) Gradually-varied flow in open channel networks, XIX IMEKO World Congress Fundamental and Applied Meteorology September 6−11, 2009, Lisbon, Portugal.

Vatankhah, A.R.(2011) Direct integration of gradually varied flow equation in parabolic channels. Flow Measurement and Instrumentation, 3, 22, 235–241.

US Army Corps of Engineers (2010) HEC-RAS hydraulic reference.